Polymer-Based Blue Electrophosphorescent Light-Emitting Diodes Using a Bisorthometalated Ir(III) Complex as the Triplet Emitter

Chang-Lyoul Lee, Rupasree Ragini Das,† and Jang-Joo Kim*

School of Materials Science and Engineering, Seoul National University, San 56-1, Shillim-Dong, Kwanak-Gu, Seoul 151-744, Korea

Received February 26, 2004. Revised Manuscript Received May 28, 2004

Polymer-based blue electrophosphorescent light-emitting diodes are reported by doping bisorthometalated (phosphine)cyanoiridium(III) complex $Ir(ppy)_2P(n\text{-}Bu)_3CN$ (ppy = 2-phenylpyridine, $P(n\text{-}Bu)_3$ = tri-*n*-butylphosphine) in poly(vinylcarbazole) (PVK) as the source of emission. The (phosphine)cyanoiridium(III) complex shows sky blue emission with two peaks at 467 and 496 nm originating from an admixture of triplet metal-to-ligand charge-transfer and ligand-centered states. The PL and EL spectra of an $Ir(ppy)_2P(n\text{-}Bu)_3CN$-doped PVK film and device exhibited no emission from PVK, indicating that the energy transfer from PVK to $Ir(ppy)_2P(n\text{-}Bu)_3CN$ is efficient. A maximum external quantum efficiency (η_{ex}) of 1.45% and power efficiency (η_p) of 0.99 lm/W were achieved at 13 and 6 mA/cm^2 at a 10 wt % doping concentration, respectively.

Introduction

Organic electrophosphorescent light-emitting diodes (LEDs) using orthometalated Ir(III) complexes emitting from their triplet metal-to-ligand charge-transfer (^{3}MLCT) states are intensively studied because of their high emission efficiency.[1,2] The phosphorescent molecules allow harvesting light not only from the singlet but also from the triplet excitons; therefore, 100% internal quantum efficiency can be achieved theoretically. High efficient electrophosphorescent LEDs have been indeed reported by doping blue to red emissive phosphorescent dyes in a low molecular weight organic host.[1−8]

Polymer electrophosphorescent LEDs are also investigated.[9−16] However, polymer electrophosphorescent LEDs show lower quantum efficiencies than LEDs consisting of small organic molecules as the host for the same phosphorescent dopant. The phase separation or aggregation of dopant is one of the reasons for the lower quantum efficiency.[11] Especially, blue polymer electrophosphorescent LEDs show relatively poor device performance compared to green and red ones. The maximum external quantum efficiency (η_{ex}) of 1.3% and power efficiency of 0.8 lm/W were achieved when FIrpic was doped in PVK host.[13] Proper selection of a polymer host and an efficient blue phosphorescence dye by structural tuning and ligand variation[17,18] will improve the quantum efficiency of blue polymer electrophosphorescent LEDs to realize the full color display.

In our previous work, we realized the blue emission by replacing one ppy unit in $Ir(ppy)_3$ by two monodentate groups as in the complexes $Ir(ppy)_2PX_3Cl$, where X = Ph and *n*-Bu.[19] The introduction of these nonorthometalating ligands with different π-accepting and electron-delocalizing abilities compared to that of the ppy ligand alters the molecular energy states in such a way that the HOMO−LUMO energy gap is increased with the achievement of the blue-shifted emission. These complexes emit in the range of 485−505 nm from the ^{3}MLCT state but are found to be thermally unstable and not very efficient when doped in PVK.

* To whom correspondence should be addressed. E-mail: jjkim@snu.ac.kr.

† Current address: Samsung Advanced Institute of Technology, San 14-1, Nongseo-ri, Giheung-eup, Yongin-si, Gyeonggi-do, Korea.

(1) Adachi, C.; Baldo, M. A.; Forrest, S. R.; Thompson, M. E. *Appl. Phys. Lett*. **2000**, *77*, 904.
(2) Fukasa, A.; Dao, K. L. T.; Kido, J. *Polym. Adv. Technol.* **2002**, *12*, 601.
(3) Adachi, C.; Baldo, M. A.; Thompson, M. E.; Forrest, S. R. *J. Appl. Phys*. **2001**, *90*, 5048.
(4) Ikai, M.; Tokito, S.; Sakamoto, Y.; Suzuki, T.; Taga, Y. *Appl. Phys. Lett.* **2001**, *79*, 156.
(5) Adachi, C.; Baldo, M. A.; Forrest, S. R.; Lamansky, S.; Thompson, M. E.; Kwong, R. C. *Appl. Phys. Lett.* **2001**, *78*, 1622.
(6) Adachi, C.; Kwong, R. C.; Djurovich, P.; Adamovich, V.; Baldo, M. A.; Thompson, M. E.; Forrest, S. R. *Appl. Phys. Lett*. **2001**, *79*, 2082.
(7) Holmes, R. J.; Forrest, S. R.; Tung, Y.-J.; Kwong, R. C.; Brown, J. J.; Garon, S.; Thompson, M. E. *Appl. Phys. Lett.* **2003**, *82*, 2422.
(8) Tokito, S.; Iijima, T.; Suzuri, Y.; Kita, H.; Tsuzuki, T.; Sato, F. *Appl. Phys. Lett.* **2003**, *83*, 569.
(9) Lee, C.-L.; Lee, K.-B.; Kim, J.-J. *Appl. Phys. Lett.* **2000**, *77*, 2280.
(10) Vaeth, K. M.; Tang, C. W. *J. Appl. Phys*. **2002**, *92*, 3447.
(11) Noh, Y.-Y.; Lee, C.-L.; Kim, J.-J.; Yase, K. *J. Chem. Phys.* **2003**, *118*, 2853.
(12) Gong, X.; Ostrowski, J. C.; Bazan, G. C.; Moses, D.; Heeger, A. J. *Appl. Phys. Lett.* **2002**, *81*, 3711.
(13) Kawamura, Y.; Yanagida, S.; Forrest, S. R. *J. Appl. Phys.* **2002**, *92*, 87.
(14) Markham, J. P. J.; Anthopoulos, T.; Magennis, S. W.; Samuel, I. D. W.; Male, N. H.; Salata, O.; Lo, S.-C.; Burn, P. L. *SID 02 Digest*. **2002**, 1032.
(15) Vaeth, K. M.; Dicillo, J. *J. Polym. Sci., Part B: Polym. Phys.* **2003**, *41*, 2715.
(16) Markham, J. P. J.; Lo, S.-C.; Magennis, S. W.; Burn, P. L.; Samuel, I. D. W. *Appl. Phys. Lett.* **2002**, *80*, 2645.
(17) Lamansky, S.; Djurovich, P.; Murphy, D.; Abdel-Razzaq, F.; Lee, H.-E.; Adachi, C.; Burrows, P. E.; Forrest, S. R.; Thompson, M. E. *J. Am. Chem. Soc.* **2001**, *123*, 4304.
(18) Brooks, J.; Babayan, Y.; Lamansky, S.; Djurovich, P. I.; Tsyda, I.; Bau, R.; Thompson, M. E. *Inorg. Chem*. **2002**, *41*, 3055.
(19) Lee, H. W.; Das, R. R.; Lee, C.-L.; Noh, Y.-Y.; Kim, J.-J. *Mater. Res. Soc. Symp. Proc.* **2002**, *708*, 119.

10.1021/cm049701b CCC: $27.50
Published on Web 07/20/2004

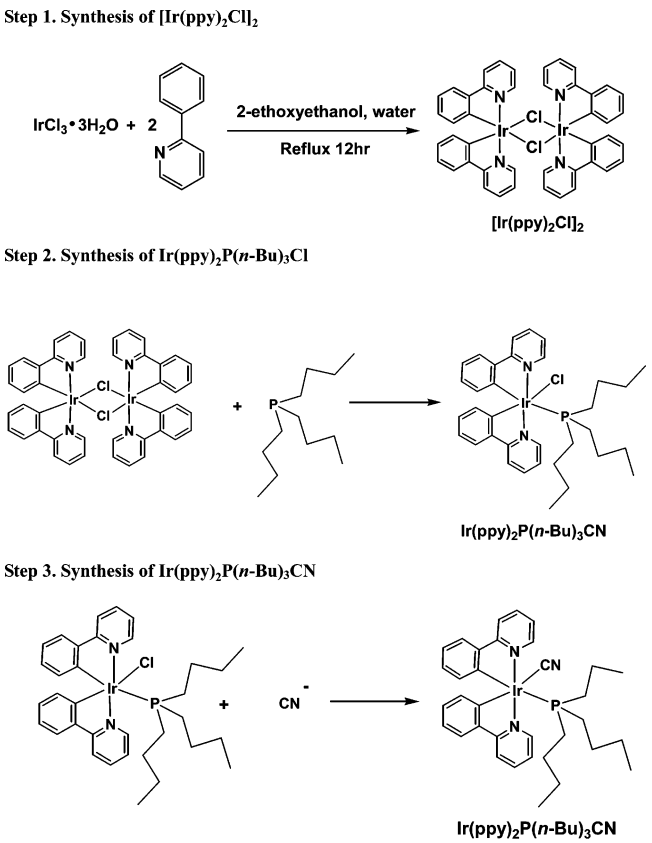

Figure 1. Synthetic scheme and molecular structure of phosphorescent dyes.

In this paper, we report a new blue phosphorescent material, cyano(bis(2-phenylpyridinato-*N*,$C^{2'}$)(tri-*n*-butylphosphine)iridium(III) complex [Ir(ppy)$_2$P(*n*-Bu)$_3$CN], by replacing the weak π donor Cl with the strong σ donor and π acceptor CN. Introduction of the CN group in the (phosphine)iridium(III) complex achieves better chemical stability and blue-shifted emission by increasing the HOMO−LUMO gap. We compare the photophysical properties of the excited states of the (phosphine)cyanoiridium(III) complex with those of the (phosphine)chloroiridium(III) complex. Finally, we report the device performances by doping the (phosphine)cyanoiridium(III) complex in the PVK host.

Experimental Section

Synthesis of Phosphorescent Dyes. Figure 1 shows the synthetic scheme and molecular structure of phosphorescent dyes Ir(ppy)$_2$P(*n*-Bu)$_3$Cl and Ir(ppy)$_2$P(*n*-Bu)$_3$CN. All syntheses were carried out in a nitrogen atmosphere using the Schlenk arrangement, and the products were stored in a vacuum to avoid air contact. The starting material [Ir(ppy)$_2$Cl]$_2$ was prepared following the literature procedure.[20] The elemental analysis and ^{1}H NMR and mass spectra characterized the synthesized materials.

Synthesis of Ir(ppy)$_2$P(n-Bu)$_3$Cl. A 0.1 mmol of the dinuclear complex [Ir(ppy)$_2$Cl]$_2$ was treated with 0.2 mmol of tri-*n*-butylphosphine in 10 mL of dichloromethane and stirred until the solution became clear. The solution was then filtered and rotary evaporated. The compound was purified by passing through a column of alumina using dichloromethane as the eluent. It was crystallized from a solution of dichloromethane and hexane (1:1). Green-yellow. Anal. Calcd: C, 55.30; N, 3.79; H, 5.83. Found: C, 55.06; N, 3.51; H, 5.57. ^{1}H NMR (300 MHz, $CDCl_3$) (ppm): 9.89 (d, 1H), 8.87 (d, 1H), 7.91−7.73 (m, 4H), 7.58−7.50 (dd, 2H), 7.19 (t, 1H), 7.10 (t, 1H), 6.86−6.74 (m, 3H), 6.67 (t, 1H), 6.40 (d, 1H), 5.89 (t, 1H), 1.53−1.46 (t, 6H), 1.21 (t, 12H), 1.08 (t, 9H).

Synthesis of Ir(ppy)$_2$P(n-Bu)$_3$CN. A 0.1 mmol sample of a solution of chlorophosphine complex in 5 mL of dichloromethane was added to 0.25 mmol of KCN in 10 mL of methyl alcohol and stirred for 30 min. The solution was then filtered and rotary evaporated. The compound was purified by passing through a column of silica using dichloromethane−acetone (95:5) as the eluent. The compound was crystallized as a pale yellow solid from a solution of dichloromethane and hexane. Anal. Calcd: C, 56.19; N, 5.78; H, 5.92. Found: C, 56.06; N, 5.54; H, 5.52. ^{1}H NMR (300 MHz, $CDCl_3$) (ppm): 9.73 (d, 1H), 8.75 (d, 1H), 7.92−7.78 (m, 4H), 7.59−7.55 (m, 2H), 7.18 (t, 1H), 7.08 (t, 1H), 6.85 (t, 2H), 6.78−6.72 (m, 2H), 6.34 (d, 1H), 6.00 (t, 1H), 1.57−1.48 (m, 6H), 1.12 (t,12H), 0.77 (t, 9H). The mass spectrum shows peaks at 728 and 527 corresponding to [Ir(ppy)$_2$ P(*n*-Bu)$_3$CN]$^+$ and [Ir(ppy)$_2$CN]$^+$.

Measurements and Device Fabrication. ^{1}H NMR spectra were recorded at 300 MHz with a JEOL JNM-LA 300 WB FT-NMR spectrometer. The chemical shifts were referenced to internal $SiMe_4$. Elemental analyses were performed using a Thermo Quest Italia S.p.A. EA1110 CHNS-O analyzer. Mass spectra (fast atom bombardment) were obtained on a JEOL JMS 700 high-resolution mass spectrometer. Absorption spectra were monitored with a Hewlett-Packard HP8452A UV−vis diode array spectrophotometer. PL spectra were detected with an ACTON spectrometer connected to a photomultiplier tube with a xenon lamp as excitation source. Cyclic voltammetry was performed with an Autolab potentiostat by Echochemie under nitrogen in a one-compartment electrolysis cell consisting of a platinum wire working electrode, a platinum wire counter electrode, and a quasi Ag^+/AgCl reference electrode. Ferrocene was used as a reference material. PL emission lifetimes were measured by a gated intensified diode array detector through a monochromator by exciting the samples at the fourth harmonic of a Q-switched Nd:YAG laser with a pulse duration of 6 ns and a repetition rate of 10 Hz at room temperature. Low-temperature PL spectra were also recorded by a gated intensified diode array detector through a monochromator at 5.5 K.[11]

The glass substrate precoated with indium−tin oxide was cleaned by an ultrasonic bath of acetone, followed by 2-propanol. Surface treatment was carried out by exposing ITO to UV ozone. The hole-injecting poly(3,4-ethylenedioxythiophene) (PEDOT) was spin coated onto the ITO with a thickness of 40 nm and baked at 120 °C for 10 min. Ir(ppy)$_2$P(*n*-Bu)$_3$CN-doped PVK solution was spin coated onto the PEDOT layer and used as the hole transport and emissive layers. The doping concentrations were 0.5−10 wt %. A 20 nm thick BCP (2,9-dimethyl-4,7-diphenyl-1,10-phenanthroline) layer was deposited as the exciton-blocking and electron-transporting layer followed by a 30 nm Alq_3 (tris(8-hydroxyquinoline)aluminum(III)) layer as an electron-transporting layer. Finally, a Mg−Ag layer (100 nm) capped by 20 nm of Ag was deposited as the cathode through a shadow mask by thermal evaporation. The fabricated multilayer polymer-based phosphorescent LEDs have the structure of ITO/PEDOT (40 nm)/PVK−Ir(ppy)$_2$P(*n*-Bu)CN (23 nm)/BCP (20 nm)/Alq_3 (30 nm)/Mg:Ag (100 nm)/Ag. The sample spot diameter is 1 mm. The light output was collected by a calibrated silicon photodiode, and the current−voltage characteristics were measured by using a Kitheley 237 source measurement unit. All the measurements were performed at room temperature in air.

Result and Discussion

Photophysical Properties. Figure 2 shows the absorption and emission spectra of 10^{-5} M solutions of Ir(ppy)$_2$P(*n*-Bu)$_3$Cl and Ir(ppy)$_2$P(*n*-Bu)$_3$CN in dichloromethane. The absorption spectra demonstrate the typical features of the transition-metal complexes with a large spin−orbit coupling constant. The absorptions below 330 nm are metal-perturbed ligand-centered

(20) Garces, F. O.; Watts, R. J. *Inorg. Chem*. **1998**, *27*, 3464.

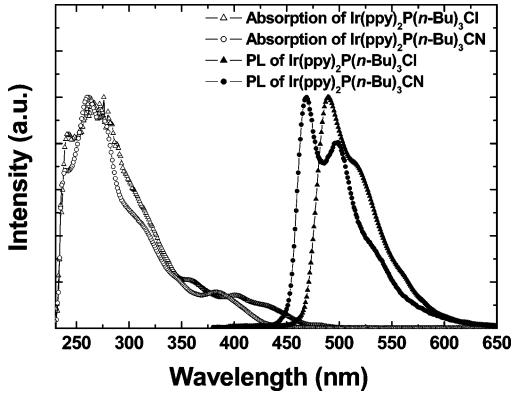

Figure 2. Absorption and emission spectra of 10^{-5} M solutions of $Ir(ppy)_2P(n\text{-}Bu)_3Cl$ and $Ir(ppy)_2P(n\text{-}Bu)_3CN$ in dichloromethane.

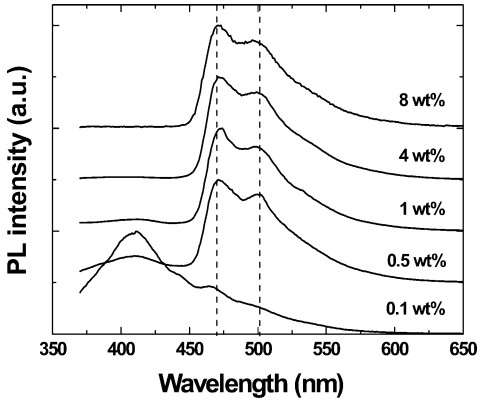

Figure 3. PL spectra of $Ir(ppy)_2P(n\text{-}Bu)_3CN$-doped PVK films with different doping concentrations.

absorptions on the basis of the high extinction coefficients of the bands, and bands higher than 330 nm are charge-transfer bands. The absorption spectrum of the chloro complex extends up to 450 nm and exhibits more resolved bands in the 370−450 nm region. These bands can be assigned as MLCT bands on the basis of the phenylpyridine ligand. The MLCT bands are blue shifted when CN replaces Cl in the (phosphine)iridium(III) complex. In the cyano complex, the ^{1}MLCT and ^{3}MLCT bands are not distinct, as shown by the broad band at ~382 nm. This is an indication of the greater ligand character in the MLCT state of the cyano complex.[17]

These (phosphine)iridium(III) complexes exhibit strong luminescence in both the powder and solution states at room temperature. The peak emission (λ_{max}) of the chloro complex is observed at 492 nm. The luminescence of $Ir(ppy)_2P(n\text{-}Bu)_3Cl$ shifts to the blue region compared to that of $Ir(ppy)_3$, indicating that the HOMO−LUMO gap is increased due to the higher ligand field strength of the phosphine.

The emission spectrum of the cyano complex shows a clear 20 nm blue shift of λ_{max} from that of the corresponding chloro complex. The ligand field strength of CN is larger due to its strong σ donor and π acceptor ability. This causes larger splitting of the d-orbital and consequently more lowering of the metal-centered HOMO. The CIE chromaticity coordinates of the cyano complex are $x = 0.16$ and $y = 0.33$ in the solution state.

Electrochemical Properties of Phosphorescent Dyes. The energy levels of the phosphine complexes were measured by cyclic voltammetry with reference to Cp_2Fe/Cp_2Fe^+. The chloro complex shows an irreversible oxidation process. But the cyano complex exhibits quasi-reversible oxidation processes. The quasi-reversible nature of these complexes reveals the MLCT nature of the electronic transitions. The HOMO levels of $Ir(ppy)_2P(n\text{-}Bu)_3Cl$ and $Ir(ppy)_2P(n\text{-}Bu)_3CN$ are found to be 5.18 and 5.46 eV, respectively. The deeper HOMO of the cyano complex demonstrates the strong σ donor and π acceptor ability of the cyano group compared to the chloro ligand.

Excited-State Lifetime of the Phosphorescent Dyes. The excited-state lifetimes of the (phosphine)iridium(III) complexes are determined using 6 wt % (phosphine)iridium(III) complex-doped PMMA films. The chloro complex exhibits a lifetime of ~1.2 μs corresponding to the peak emission (492 nm). However, the lifetimes corresponding to the two separate emission peaks of the cyano complex are about 4 μs (4.12 μs at 467 nm, 4.27 μs at 496 nm). The longer lifetimes of the cyano complex indicate more ligand character in the MLCT state of the complex.[18]

PL and EL Spectra of $Ir(ppy)_2P(n\text{-}Bu)CN$-Doped PVK Films and Devices. Figure 3 shows the PL spectra of $Ir(ppy)_2P(n\text{-}Bu)_3CN$-doped PVK films with different doping concentrations. Emission from PVK was mostly quenched when the doping concentration was over 1 wt %, indicating that the Förster energy transfer is efficiently taking place above a 1 wt % doping concentration.

Figure 4a shows the EL spectra of the $Ir(ppy)_2P(n\text{-}Bu)_3CN$-doped PVK device with different doping concentrations. The EL spectrum of the $Ir(ppy)_2P(n\text{-}Bu)_3CN$-doped PVK device is similar to the PL spectrum of the $Ir(ppy)_2P(n\text{-}Bu)_3CN$-doped PVK film. The emission at 440 nm could be due to the emission from the hole-blocking BCP. In the bilayer device, ITO/PEDOT/$Ir(ppy)_2P(n\text{-}Bu)_3CN$:PVK (8 wt %)/Mg:Ag/Ag, no emission at 440 nm was observed. The emission at 440 nm originating from BCP can be removed by increasing the doping concentration of the cyano complex as shown in Figure 4a.

Interestingly enough, the relative emission intensity at 467 nm to that at 496 nm is lowered in the EL spectrum compared to the PL spectrum with increasing applied voltage as shown in Figure 4b. The emission process and the resulting spectrum depend on the overlap of the vibrational-state wave function of the excited and ground states and nuclear distances in the excited state. In general, the nuclear distances of the molecule in the excited state are different from those in the ground state. These nuclear distances can be affected by the environment of the excited state. The higher PL intensity at the shorter vibronic peak indicates that the ^{3}MLCT state of the cyano complex has almost the same nuclear distance as the ground state when the cyano complex is excited by direct optical excitation or singlet energy transfer from the host PVK.

However, under electrical excitation, the electronic charge distribution of the cyano complex at the excited state can be changed due to the applied electric field and/or positive and negative polarons surrounding the complex. The highly polarizing moiety of CN is expected to give nonlinear polarization to the applied or local

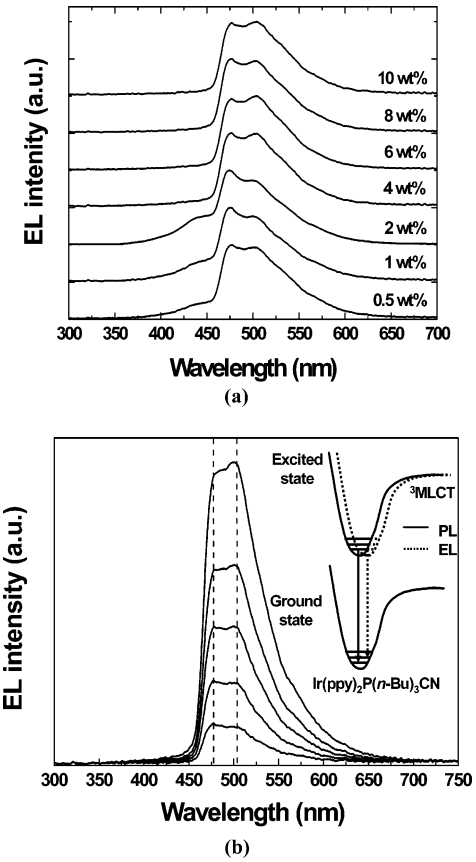

Figure 4. (a) EL spectra of Ir(ppy)$_2$P(*n*-Bu)$_3$CN-doped PVK devices with different doping concentrations. The applied voltage was 14 V. (b) EL spectrum of an 8 wt % Ir(ppy)$_2$P(*n*-Bu)$_3$CN-doped PVK device versus applied voltage (13, 15, 17, 19, and 21 V from bottom to top). Inset: energy diagram of Ir(ppy)$_2$P(*n*-Bu)$_3$CN.

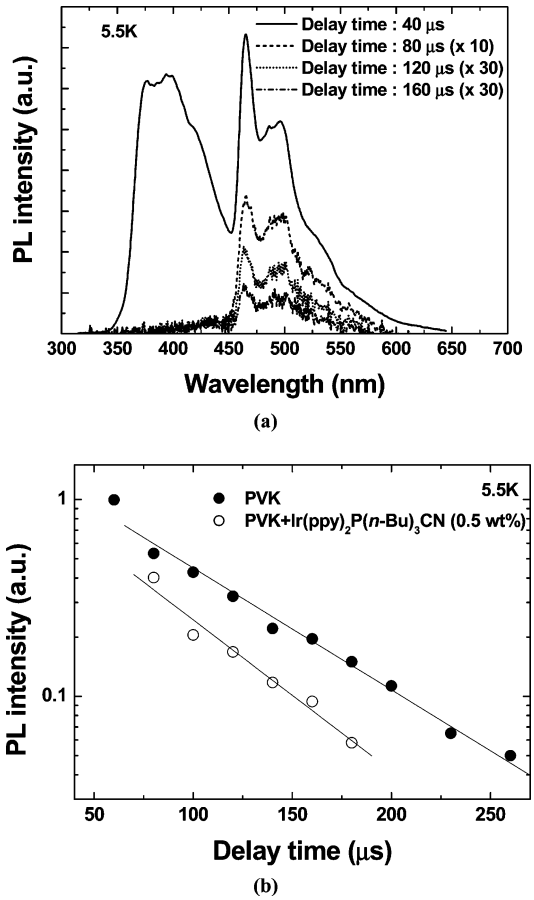

Figure 5. (a) Low-temperature (5.5 K) PL spectrum of a 0.5 wt % Ir(ppy)$_2$P(*n*-Bu)$_3$CN-doped PVK film at different delay times. (b) Comparison of the decay profiles of the triplet exciton of PVK and PVK doped with Ir(ppy)$_2$P(*n*-Bu)$_3$CN (0.5 wt %).

electric field. Such an effect can result in different nuclear configurations in the excited state from the optical excitation, and the nuclear distance in the electronic excited states is different from that in the ground state. This leads to the electronic transition from the lowest vibrational state of the electronic excited state to the second lowest vibrational state of the ground state of the cyano complex becoming the most probable transition. This speculation is supported by the gradual change of the intensity ratio with the applied electric field. This process is explained in the inset of Figure 4b. The CIE chromaticity coordinates of the EL spectrum of the Ir(ppy)$_2$P(*n*-Bu)$_3$CN-doped PVK device shift to $x = 0.22$ and $y = 0.40$ at 13 V from $x = 0.16$ and $y = 0.33$ for solution PL due to the spectrum change.

Energy Transfer and Device Performance of Ir(ppy)$_2$P(*n*-Bu)CN-Doped PVK LEDs. The host PVK has a lower triplet energy (2.46 eV with a peak wavelength of 502 nm)[11] than the guest Ir(ppy)$_2$P(*n*-Bu)$_3$CN (2.65 eV) so that an endothermic energy transfer from the host triplet to the dopant triplet is anticipated.[6,13] Low-temperature PL spectra of the 0.5 wt % Ir(ppy)$_2$P(*n*-Bu)$_3$CN-doped PVK film with different delay times (Figure 5a) give evidence of triplet−triplet energy transfer between PVK and the cyano complex. Since the lifetime of the triplet excited state of Ir(ppy)$_2$P(*n*-Bu)$_3$CN is about 4 μs, the delayed emission from Ir(ppy)$_2$P(*n*-Bu)$_3$CN on the time scale of 100 μs must originate from the triplet energy transfer from the PVK host. It must be noted that the singlet lifetime of PVK is on the order of nanoseconds and the emission in the range of 350−450 nm is the delayed fluorescence from PVK.[11]

Further evidence of the energy transfer is provided from the comparison of the decay profile of the triplet exciton of PVK with and without doping of Ir(ppy)$_2$P(*n*-Bu)$_3$CN. If triplet energy transfer takes place from the host to the guest in the system, the triplet lifetime of the host will shorten by doping because of the opening of the fast decay channel. Unfortunately, direct comparison of the decay profiles is not possible in this system because the triplet emission spectrum of PVK overlaps with the emission spectrum of Ir(ppy)$_2$P(*n*-Bu)$_3$CN. However, since the emission from Ir(ppy)$_2$P(*n*-Bu)$_3$CN in PVK at a delay time longer than tens of microseconds originates from the energy transfer from the triplet exciton in PVK and its intensity is proportional to the number of triplet excitons of PVK, the decay profile of Ir(ppy)$_2$P(*n*-Bu)$_3$CN emission in PVK reflects the decay profile of PVK triplet excitons in the doped film. The proportionality is based on the fact that the energy transfer is the first-order kinetic process if the number of Ir(ppy)$_2$P(*n*-Bu)$_3$CN molecules in the ground state is constant, i.e., the number of Ir(ppy)$_2$P(*n*-Bu)$_3$CN molecules in the excited state is much smaller than in the ground state.

Figure 5b shows the decay profiles of PVK triplet excitons with and without[11] the doping of Ir(ppy)$_2$P(*n*-Bu)$_3$CN. The triplet lifetime of PVK was reduced

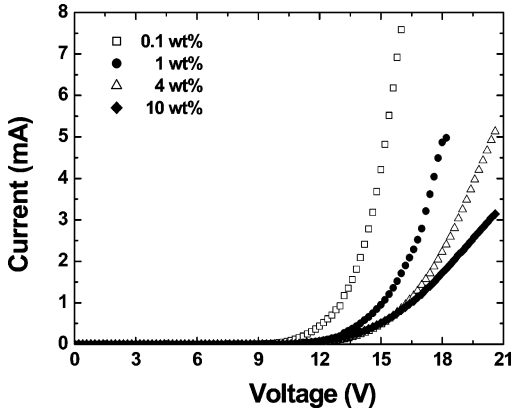

Figure 6. Current density vs voltage characteristics of $Ir(ppy)_2P(n\text{-}Bu)_3CN$-doped PVK devices as a function of doping concentration.

from 76 to 56 μs by doping of 0.5 wt % $Ir(ppy)_2P(n\text{-}Bu)_3CN$ in PVK, indicating that the triplet energy transfer takes place. The decay of the delayed fluorescence of PVK in the doped film is much faster than the decay of $Ir(ppy)_2P(n\text{-}Bu)_3CN$ emission because the delayed fluorescence is the second-order kinetic process of the triplet excitons of PVK.

Not only the singlet and triplet energy transfer but also charge confinement is operating in the devices as evidenced by the increment of driving voltage with increasing doping concentration. Figure 6 shows the current density versus voltage characteristics of $Ir(ppy)_2P(n\text{-}Bu)_3CN$-doped PVK devices as a function of doping concentration. The turn-on voltage of $Ir(ppy)_2P(n\text{-}Bu)_3CN$-doped PVK devices increases with increasing doping concentration. The increment of the device turn-on voltage is consistent with charge trapping, especially holes with regard to energy level arrangements of the $Ir(ppy)_2P(n\text{-}Bu)_3CN$ molecules. Thus, the various mechanisms (singlet and triplet energy transfer and charge recombination on the dopant site) contributed to the emission process of PVK:$Ir(ppy)_2P(n\text{-}Bu)_3CN$ LEDs.

Figure 7 shows the (a) external quantum efficiencies and (b) luminance of the $Ir(ppy)_2P(n\text{-}Bu)_3CN$-doped PVK devices versus the current density with different doping concentrations. The device furnishes a maximum external quantum efficiency (η_{ex}) of 1.45% and power efficiency (η_p) of 0.99 lm/W at a 10 wt % doping concentration. A peak luminance of 6800 cd/m^2 is achieved at 400 mA/cm^2 (20.6 V). In contrast to organic electrophosphorescent LEDs showing a fast decrease of the quantum efficiency (η_{ex}) with increasing current density, our polymer electrophosphorescent LEDs showed little roll-off of the quantum efficiency at higher current density. The reason behind the low roll-off of the quantum efficiency of the device is not clear yet, and it is under investigation now.

The replacement of Cl by CN in the (phosphine)-iridium(III) complex achieves higher device performance. For the comparison of the device performance of the chloro and cyano complexes, bilayer devices with the configuration of ITO/PEDOT/PVK:phosphine complexes (8 wt %)/Mg:Ag/Ag were fabricated. A maximum external quantum efficiency (η_{ex}) of 0.007% at 138 mA/cm^2 (12.2 V) and a peak luminance of 22 cd/m^2 are achieved at 1440 mA/cm^2 (18 V) for the chloro complex. The device with the cyano complex furnished a maximum external quantum efficiency (η_{ex}) of 0.3% at 23 mA/cm^2 (11.2 V) and a peak luminance of 980 cd/m^2 at 210 mA/cm^2 (16.2 V).

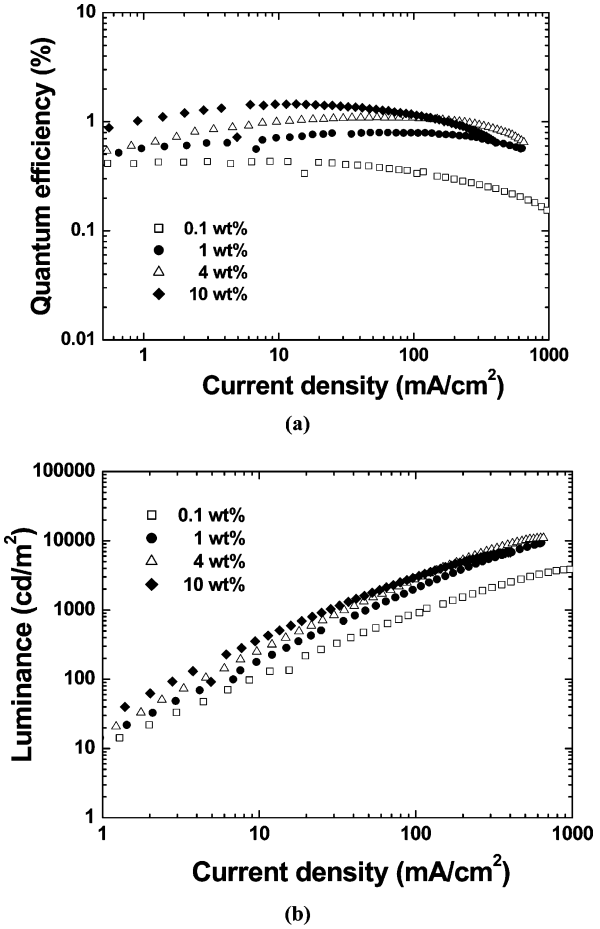

Figure 7. (a) External quantum efficiencies (η_{ex}) of the $Ir(ppy)_2P(n\text{-}Bu)_3CN$-doped PVK devices versus the current density at different doping concentrations. (b) Luminance versus current density of the $Ir(ppy)_2P(n\text{-}Bu)_3CN$-doped PVK devices.

The device performance is expected to be improved by the purification of the constituent materials, and measurement in an inert environment, because endothermic energy transfer can be seriously interrupted by nonradiative defect states such as oxygen or water.[6] And also use of a polymer host of higher triplet energy than the dopant as the organic electrophosphorescent LED could[7,8] also increase the device performance.

Conclusion

In summary, the bisorthometalated monochloro- and -cyano(phosphine)iridium(III) complexes were synthesized, and the effects of the phosphine and cyano groups on the photo- and electrophysical properties of the complex were studied. The cyano complex shows sky blue emission with two peaks at 467 and 496 nm and is photostable. A maximum external quantum efficiency (η_{ex}) of 1.45% and power efficiency (η_p) of 0.99 lm/W were achieved at 13 and 6 mA/cm^2 at a 10 wt % doping concentration, respectively.

Acknowledgment. This work was financially supported by CRM-KOSEF, Korea University, and Dongwoo Fine-Chem Co., Ltd. R.R.D. is thankful to the government of Orissa, India, for granting a study leave.
CM049701B